Les Cahiers du GERAD ISSN: 0711–2440

Global asset optimization of open pit mining complexes under uncertainty

R. Goodfellow
R. Dimitrakopoulos

G–2014–55

August 2014

GERAD HEC Montréal
3000, chemin de la Côte-Sainte-Catherine
Montréal (Québec) Canada H3T 2A7

Tél. : 514 340-6053
Téléc. : 514 340-5665
info@gerad.ca
www.gerad.ca

Global asset optimization of open pit mining complexes under uncertainty

Ryan Goodfellow

Roussos Dimitrakopoulos

GERAD & COSMO – Stochastic Mine Planning Laboratory, Department of Mining and Materials Engineering, McGill University, Montréal (Québec) Canada H3A 0E8

ryan.goodfellow@mail.mcgill.ca
roussos.dimitrakopoulos@mcgill.ca

August 2014

Les Cahiers du GERAD

G–2014–55

Abstract: Global asset optimization aims to simultaneously optimize mine production schedules, destination policies and the various processing streams in order to maximize the economic value over the life of a mineral resource supply chain. Conventional mine optimization approaches are incapable of incorporating geological uncertainty and may lead to severe deviations from forecasted production targets. Stochastic optimization models that manage risk in mine design and production scheduling have been developed over the past several years, however these models are often oversimplified, thus limited to provide only a local optimum in terms of the mining complex as a whole.

This paper addresses the issue of global optimization of open pit mine production schedules for complex mining supply chains under geological uncertainty. The proposed simulation-optimization framework builds on previous mining supply chain optimization work by permitting extraction decisions to be made simultaneously with material destination policies and processing stream decisions in order to maximize the value of the supply chain. The resulting framework is capable of modelling and efficiently optimizing over the non-linear intricacies that are often present in large mining complexes. The proposed optimizer uses a hybrid of both simulated annealing and particle swarm optimization. The method is tested on a copper-gold deposit and experimental results demonstrate that the optimizer is capable of generating production schedules and destination policies that reduce the risk of meeting production targets, have 14% higher net present value and increase the size of the final pit by 22%.

Key Words: Open pit mine design, supply chain optimization, production scheduling, metaheuristics, destination policy.

1 Introduction

A mining supply chain maps a spatio-temporal flow of materials from open pit or underground mines through various processing streams and destinations to final saleable products. Global asset optimization (Whittle, 2007; Whittle, 2009) aims to optimize mining supply chains, starting from the decisions of what material to extract from the various sources (mines) in a given time period, and how to best utilize the supply chain's resources to maximize the value of the material that has been extracted. Historically, these two components have been optimized independently, leading to sub-optimal solutions for the supply chain as a whole. Existing attempts at global asset optimization ignore the compounded effect that uncertainty (i.e. geological or economic) has on the value and operational feasibility of the supply chain (Monkhouse and Yeates, 2007). As the complexity of the supply chain increases in terms of number of mines, destinations and processing stream options, there is an increasing importance in solving all elements simultaneously while considering the uncertainty that arise within the mining complex's various components.

A substantial amount of progress has been made over recent years in order to integrate geological, or supply, uncertainty into open pit mine production scheduling optimization models. Ramazan and Dimitrakopoulos (2012) propose a two-stage stochastic integer programming (SIP) formulation (Birge and Louveaux, 1997) that seeks to maximize the net present value (NPV) of a production schedule while simultaneously minimizing the risk of not meeting production targets. Through the use of a parameter referred to as geological risk discounting (Dimitrakopoulos and Ramazan, 2004), the authors force the optimizer to strike a balance between extracting high value and low-risk material at the beginning of a mine's life, while deferring riskier material to later periods when more geological information is available. The basic SIP model has been tested and improved over time (Leite and Dimitrakopoulos, 2007; Jewbali, 2006; Benndorf and Dimitrakopoulos, 2009; Albor and Dimitrakopoulos, 2010; Lamghari and Dimitrakopoulos, 2012a), and the results consistently demonstrate that the NPV of the production schedule that considers geological uncertainty can be substantially higher than that of a conventional schedule, and, moreover, there is substantially less risk in terms of deviations from production targets. Despite these advances in integrating geological uncertainty into mine production scheduling models, all of the previous formulations make two limiting assumptions: first, the definition of ore and waste are defined a-priori, hence cut-off grade optimization (Lane, 1988; Rendu, 2008) is not directly integrated in the models, and finally, the previous models assume a simple supply chain that consists of a processing facility (mill) and a waste dump, without any consideration for intermediate or subsequent destinations.

To address issues related to simultaneous cut-off grade optimization with open-pit production scheduling, Boland et al. (2009) propose a multistage stochastic programming model that allows processing decisions to be made dynamically (per simulation), along with mining extraction decisions that can adapt as uncertainty is revealed as mining progresses. While being an interesting concept, this method suffers from the flaw that the optimizer returns several mine design possibilities, which is often impractical for a mine engineer who needs to use these designs for subsequent work. The authors also rely on the time-separable properties of the formulation, which makes it challenging to integrate more advanced processing streams in the model (e.g. stockpiles). Moreover, scenario-dependent destination policies are overly optimistic and don't reflect the fact that destination decisions (such as cut-off grade policies) need to be decided while considering the geological uncertainty. Menabde et al. (2007) propose a mixed integer programming (MIP) model that integrates geological uncertainty into production scheduling while simultaneously generating robust cut-off grade policies. The authors note an increase in NPV when permitting the optimizer to select the cut-off grade versus the case when only the marginal cut-off is used. This model, however, doesn't explicitly attempt to control the risk over the life of the mine.

To address issues related to more complex supply chains, Ramazan and Dimitrakopoulos (2004) introduce a stockpile into the SIP model. This model suffers the same a-priori cut-off grade limitation from previous SIP models, but also suffers from having to specify the average stockpile grade a-priori in order to preserve linearity for the model. Lamghari and Dimitrakopoulos (2012b) design an efficient metaheuristic based on this model, and De Frietas Silva et al. (2013) improve the method by successively solving the model and updating the stockpile grades, however the method cannot be easily extended to cases with stockpile capacities and grade blending or more complex supply chains.

While the methods for integrating geological uncertainty into long-term production scheduling have undergone considerable advances, they are not presently capable of optimizing while considering complex destination policies and processing streams. The underlying issue with these optimization problems is the extensive amount of non-linearity that is required to accurately model the blending of materials and the complex transformations from input to output products. There have been several attempts to model and optimize the various aspects of the supply chain with an increasing level of detail (Hoerger et al., 1999; Hoerger et al., 1999; Chanda, 2007; Whittle, 2007; Whittle, 2009; Bley et al., 2012), however all models ignore geological uncertainty, and are limited in the degree of flexibility in modelling the non-linear intricacies in the supply chain. Bodon et al., (2009) and Sandeman et al. (2010) present a discrete event simulation-optimization framework, which permits a high-degree of flexibility in modelling the supply chain and independent stochastic events at the various destinations, however requires simplifications to eliminate non-linear constraints. Simulation-optimization frameworks are useful tools when optimizing complex supply chains because it permits the dynamic evaluation (simulation) of the impact that a set of decisions (e.g. production schedules, destination policies and processing streams) have on a mining complex, and then attempts to improve these decisions through the use of an optimizer. More recently, Goodfellow and Dimitrakopoulos (2012) propose a simulation-optimization framework that not only permits a high degree of flexibility for modelling the non-linear aspects of the supply chain, but does not require simplifying assumptions to generate high-quality optimization solutions. Moreover, the proposed model can integrate geological uncertainty directly and can be used to generate robust destination policies.

This paper improves on the previous simulation-optimization framework by enabling the optimizer to make production scheduling decisions in addition to destination policies and processing stream decisions. First, an overview of the modelling approach proposed by Goodfellow and Dimitrakopoulos (2012) is given. Following this, a two-stage SIP formulation is proposed, where the first stage decisions are to optimize multi-mine long-term production schedules and robust destination policies, and the second-stage recourse decisions are used to optimize the various processing streams of the supply chain. Following this, the proposed solution method is discussed, which is a hybrid of particle swarm optimization and an adapted version of simulated annealing designed to handle multiple neighbourhoods. The method is then tested at on a copper-gold deposit data set. Finally, conclusions and future work are presented.

2 Stochastic global asset optimization

The goal of global asset optimization (Whittle, 2007; Whittle, 2009) is to generate a long-term (multi-) mine production schedule that provides the appropriate types, quantities and quality of materials that maximize the long-term value of the supply chain. For the sake of continuity in the descriptions from previous work, the aspect of making extraction decisions for a mine will be referred to as "production scheduling", whereas optimizing the destination policies and processing streams according to a given production schedule will be referred to as "supply chain optimization" (Goodfellow and Dimitrakopoulos, 2012). Global asset optimization simultaneously considers both production scheduling and supply chain optimization, acknowledging the interdependence of the two concepts. In this section, the proposed framework for modelling and simulating (evaluating) supply chains will be outlined. Following this, an optimization formulation for global asset optimization is given, similar to that given by Goodfellow and Dimitrakopoulos (2012), but with additional emphasis on integrating production scheduling. A description of the hybrid metaheuristic algorithms used to solve the optimization problem is then discussed.

2.1 Modelling and simulating mining supply chains

2.1.1 Background and definitions

Consider a set of locations in a mining supply chain, $L = L_m \cup L_d$, whereby $l_m \in L_m$ is used to denote a mine m from the set of mines that supply the chain with material, and $l_d \in L_d$ is used to denote a destination d from the set of destinations (e.g. concentrators, refineries, ports, customers). Consider a topologically sorted directed acyclic graph that represent the general flow of materials through a supply chain, $G^{TS}\left(L, O^{mat}_{l,l'}\right)$, where the vertices of the graph $l \in L$ are locations in the supply chain, and are connected to other vertices

(locations) $l' \in L, l \neq l'$ by a set of arcs defined in the set $O^{mat}_{l,l'}$. For the purpose of simplifying the explanation of the proposed methodology, it is assumed that this supply chain graph $G^{TS}\big(L, O^{mat}_{l,l'}\big)$ is static through time, however, in the implementation a node $l \in L$ may or may not have an arc to location l' when comparing one time period to another – a case that may arise when a mine or processing facility starts or closes. The arcs in $O^{mat}_{l,l'}$ are used to describe the flow of an output material (or product) mat from destination l, which serves as an input material at destination l'. Any destination can have multiple output materials that go to the same destination and a destination may have the same input material coming from multiple sources (e.g. multiple mines produce a similar oxide material sent to a processing plant). It is assumed that there is not a material flow from a location to the mines, i.e. $O^{mat}_{l \in L, l' \in L_m} = \emptyset$. Any destination in the supply chain $l_d \in L_d$ may receive a set of materials from a previous destination, which can then be transformed and combined into intermediate and output products.

In the proposed framework, the materials have no practical meaning, and are merely an abstraction to define the flow of materials. Properties are associated with materials and are used to give a material their meaning in the practical sense. For example, a mine may send a sulphide material to a processing plant, with a property that the represents the tonnage of a metal. More formally, each material $mat \in Mat_l$ for location $l \in L$, has an associated set of properties R_{mat_l}, whereby an individual property from the set is denoted by $r_{mat} \in R_{mat_l}$ with a value of $v^p_{r_{mat}}$ in period p. In the sorted supply chain graph, $G^{TS}\big(L, O^{mat}_{l,l'}\big)$, it is assumed that the properties associated with material mat are linearly additive. In practice, this means that if destinations $l_1 \in L$ and $l_2 \in L, l_1 \neq l_2$ both send an output material mat to destination l', the total value of the input property at l' is equal to the sum of the values coming from l_1 and l_2. While this may initially appear to be counter-intuitive, the practical reason for this is simple: if two mines are sending sulphide material to a plant, it makes sense to add the copper tonnages and total tonnages from each mine, however it is illogical to add the respective grades together.

Within any given destination in the supply chain, the transformation of materials $mat \in Mat_l$ can be modelled from inputs to intermediate products to outputs using a topologically sorted directed acyclic graph within destination l, similar to that of the supply chain graph $G^{TS}\big(L, O^{mat}_{l,l'}\big)$. Unlike the properties associated with the materials in the supply chain graph, the properties associated with intermediate or output materials can be expressed linearly or non-linearly as functions of other properties previously defined. This permits being able to model the transformation from one product into another; one example might be to convert the input copper tonnes and total tonnes into a copper head grade, which can then be used to obtain a recovery from a non-linear and non-additive grade-recovery curve. Alternatively, some non-linear transformation models can be accommodated by treating incoming materials independently (to preserve the linearly additive property), then applying non-linear transformations to combine the two materials and their respective properties (e.g. a variable throughput that may depend on the proportions of the total quantities of the various input materials).

Given that there is a natural ordering when evaluating the properties for any destination $l \in L_d$, consider a topologically sorted directed acyclic graph $G^{TS}\left(R_l, A_{r_i} A_{r_j}\right)$. The vertices are defined by $R_l = \bigcup_{mat \in Mat_l} R_{mat_l}$, i.e. all properties that must be evaluated for all materials at destination l and the arcs, $A_{r_i} A_{r_j}$, are used to describe the precedence relationship that a property $r_i \in R_l$ must be evaluated prior to evaluating $r_j \in R_l$. The result is a graph that gives the order of evaluation for the properties at a given destination, which is used when simulating the supply chain and will be discussed in Section 2.1.3.

2.1.2 Destination policies under uncertainty

A mine $l_m \in L_m$ is generally represented as a three-dimensional volume discretized by a set of blocks, B_{l_m}, where each block in the set can be denoted by $b^{l_m}_k \in B_{l_m}$ if the variable $k \in \{1, \ldots, N_{l_m}\}$ is used to index each of the N_{l_m} blocks in the model. Consider a finite set of geological simulations of the orebody, which can be indexed by $s \in \{1, \ldots, S_m\}$, where S_m is the total number of simulations available for mine l_m. In each simulation, each block contains a material type (used to define a set of potential destinations), and properties related to the material, which is simply inherited from the available material types and properties associated with mine l_m. It is noted that these material types can vary between simulations, along with

the associated property values $v^k_{r_{mat}}(s)$, which is used to denote the value of block k for property r_{mat} in simulation $s \in \{1, \ldots, S_m\}$.

There are three conceivable options regarding making decisions under uncertainty about the destination of a block. The first option is to optimize where to send the block for each simulation, an assumption made by Boland et al. (2009), which implies that the optimizer or decision-maker has perfect knowledge of the block's properties, and all other block properties in the model. Under this assumption, the optimal solutions of a supply chain optimizer (ignoring the production scheduling aspect) would be referred to as the wait-and-see solution (Birge and Louveaux, 1997), which doesn't reflect the fact that the decisions related to supply chain optimization need to be made under uncertainty. The next conceivable option is to decide on a single destination for each block (Montiel and Dimitrakopoulos, 2012); given that the material types, hence candidate destinations, may differ from one geological simulation to the next, this solution is likely to generate misclassification errors, and doesn't necessarily reflect a mine's ability to change the destination decision of the block once the block is available for extraction and has been sampled. A fair compromise between these two options to utilize classification: rather than deciding on the (possibly erroneous) block destination, one may wish to classify the blocks into groups of similar *types* of properties and make decisions that apply across all simulations (Goodfellow and Dimitrakopoulos, 2012). This concept can be used to create a destination policy based on the multi-dimensional properties of the blocks that not only eliminates misclassification, but integrates geological uncertainty into the supply chain optimization by applying the same policy across all simulations. In the case where a single property is considered (i.e. metal grade), the proposed clustering method is similar to the robust cut-off grade policies proposed by Menabde et al. (2007).

To classify the blocks over all simulations, the k-means++ (Arthur and Vassilvitskii, 2007) variant of the k-means algorithm (Lloyd, 1982) is used, which is a heuristic algorithm that attempts to find the cluster center locations such that the Euclidean distance between the cluster center and the cluster's membership blocks is minimized. Consider a subset of the blocks $B^{mat}_l \subseteq B_l$ for a mine $l \in L_m$ that are of material type $mat \in Mat_l$ for any simulation. Each material can be aggregated into $n^{l,mat}_{clusters}$ clusters, where each cluster center is defined by a set of multi-dimensional positions based on the average value of the properties, $v^k_{r_{mat}}(s)$, of the blocks that are closest to the cluster center. This implies that the membership of a given block and simulation can only belong to a single cluster, however the cluster membership may vary for each block between simulations, given that the material types and property values can vary between the simulations. For future notation when discussing production scheduling, let $clus^l_{mat,n}(s) \subseteq \{1, \ldots, N_{l_m}\}$ be used to denote the indices of the blocks from mine l that have material type mat in simulation s that are members of cluster n.

There are several advantages over other methods when using clusters to generate destination policies. The clusters act as a catalyst that enables destinations policies to be made while considering geological uncertainty, which can then be easily tested against a different set of geological simulations of the same deposit in order to verify the robustness of a solution. By moving from block destinations to cluster destinations, the issue of misclassification is eliminated, and moreover, the number of decision variables required is reduced from N_{l_m}, the number of blocks in mine l_m, to $\sum_{p \in P} \sum_{mat \in M_l} n^{l,mat}_{clusters}$, where P is the set of periods that the mine is active. For example, in a case study for a nickel laterite deposit, Goodfellow and Dimitrakopoulos (2012) reduce the number of block decision variables from 55,622 to 3,268 destination policy variables. The reader is encouraged to refer to this paper for an in-depth analysis of the impacts clustering has on the quality of the solution and computing times.

Recall that in Section 2.1.1, it is stated that the properties travelling from a source to a destination are considered to be linearly additive; as a result, a substantial amount of the data can be pre-processed for each cluster. Let $v^i_{r_{mat}}$ represent the value of property r_{mat} for a block i whose block index is a member of $clus^l_{mat,n}(s)$. Additionally, let the variable $x_{i,t} \in \{0, 1\}$ define whether or not block i is scheduled to be extracted in period t. The property value $v^t\left(clus^l_{mat,n}(s)\right)$ of cluster $clus^l_{mat,n}(s)$ can be calculated as follows:

$$v^t\left(clus^l_{mat,n}(s)\right) = \sum_{i \in clus^l_{mat,n}(s)} v^i_{r_{mat}} \cdot x_{i,t} \tag{1}$$

2.1.3 Supply chain simulation

There are three key decision variables that enable the supply chain simulation-optimization framework. First, the decision of whether or not to extract block $i \in \{1, \ldots, N_{l_m}\}$ from mine $l_m \in L_m$ in period t is defined as $x_{i,t} \in \{0, 1\}$. These variables define the production schedule, hence, the quantities and properties of the materials available for the supply chain for any given period and simulation. Secondly, let $z_d^t\left(clus_{mat,n}^l\right) \in \{0, 1\}$ be a binary decision variable that represents whether or not cluster n of material $mat \in Mat_l$ from mine $l \in L_m$ is sent to destination $d \in L_d$ in period t, where the option of going from l to d is defined in the supply chain graph $G^{TS}\left(L, O_{l,l'}^{mat}\right)$. In order to preserve resource constraints, it is required that the material from the cluster be entirely sent to a single destination, i.e. $\sum_{d \in L_d} z_d^t\left(clus_{mat,n}^l\right) = 1$. In order to define what occurs in the remainder of the processing streams of the supply chain, let the variable $y_{d'}^{t,s}\left(mat_{l_d}\right) \in [0, 1]$ represent the linear proportion of output material $mat_l \in Mat_l$ being sent from destination $l_d \in L_d$ to destination $d' \in L_d \backslash l_d$ in simulation $s \in \left\{1, \ldots, S^{total}\right\}$ and period t. Recall that the supply chain may contain multiple sources of uncertainty (geological, metal price, etc.), hence S^{total} is defined as the product of the number of simulations from all sources of uncertainty. For example, if the supply chain consists of 2 mines, each having 20 geological simulations, along with 30 metal price simulations, $S^{total} = 20^2 \cdot 30 = 12000$. In the proposed framework, it is assumed that the destination policies are applied across all simulations $s \in \left\{1, \ldots, S^{total}\right\}$, however once the material is received at the initial set of destinations after the mine, the uncertainty of the material received (and possibly other sources, such as metal price) for a given production period is revealed, and the $y_{d'}^{t,s}\left(mat_{l_d}\right)$ variables are used to decide how to make best use of the materials sent under the destination policy to maximize the value of the supply chain. For a stochastic optimization formulation, the destination policies are therefore referred to as the first-stage decision variables, and the processing proportion variables are referred to as the recourse variables (Birge and Louveaux, 1997). While it is sensible to assume that the uncertainty of a mined material is revealed when it is sent to its initial destination, it may not always be practical to make this assumption for other variables if the time of a material spent in a supply chain is long (e.g. when considering metal prices, if material is extracted in the first period, but not sold until the subsequent period). Future work may focus on a multistage framework where the uncertainty can be revealed at different positions in the supply chain, rather than simply the first destination after the mines, which would require a method to cluster some of the $y_{d'}^{t,s}\left(mat_{l_d}\right)$ proportion variables together based on the properties of the output material.

Any destination $d \in L_d$ has the option to carry over material from one period to the next; this is frequently seen in strategic stockpiles, where material is sent out to a processing facility over time. Other destinations, however, may need to preserve mass balancing requirements in order to guarantee that all output material that is available is sent out. Let D_{mat_d} represent the set of candidate destinations for output material mat_d at destination d. In the case where material is permitted to be carried over between periods, let $\sum_{d' \in D_{mat_d}} y_{d'}^{t,s}\left(mat_d\right) \leq 1$. In the case where all output material must go to the subsequent destination, let $\sum_{d' \in D_{mat_d}} y_{d'}^{t,s}\left(mat_d\right) = 1$.

For a set of given variables $z_d^t\left(clus_{mat,n}^l\right) \in \{0, 1\}$ and $y_{d'}^{t,s}\left(mat_{l_d}\right)$, the simulation of a mining supply chain proceeds as follows:

1. Based on the current production schedule for the various mines $l_m \in L_m$ defined by $x_{i,t}$, evaluate Eq. (1) to get the property values for each cluster in each time period and simulation for all mines.
2. For each simulation s and cluster $clus_{mat,n}^l(s)$, send (or update) the linearly additive properties, $v^t\left(clus_{mat,n}^l(s)\right)$, to the mine for all periods t. This step is only necessary if one wishes to impose constraints at the mine-level (e.g. mining extraction capacity) or track information about specific types of material (e.g. total quantity of sulphides versus oxides extracted).
3. For each simulation s and cluster $clus_{mat,n}^l(s)$, send (or update) the linearly additive properties, $v^t\left(clus_{mat,n}^l(s)\right)$, to the destination where $z_d^t\left(clus_{mat,n}^l\right) = 1$ for all periods t.
4. For each destination $d \in L_d$ that was updated in Step 1, evaluate the sorted property graph $G^{TS}(R_d, A_{r_1} A_{r_2})$ to transform the properties from inputs to outputs.
5. For each destination d evaluated in the previous step, each simulation and each period $t \in T_d$ (each period that d is available from lowest to highest):

(a) Send $y_{d'}^{t',s}(mat_d)$ amount of output material to destination d', in period t. Given that all properties associated with output material mat_d are assumed to be linearly additive, the quantity sent for property $r_{mat_d} \in R_{mat_d}$ is equal to $v_{r_{mat}}^{t}(s) \times y_{d'}^{t,s}(mat_d)$.

(b) If destination d permits carrying over material over time (e.g. a strategic stockpile), any remaining material that has not been sent out to subsequent destinations is added to the property value in the subsequent available period t': $v_{r_{mat}}^{t'}(s) += \left(1 - \sum_{d \in D_{mat}} y_{d'}^{t,s}(mat_d)\right) \cdot v_{r_{mat}}^{t,s}(mat_d)$.

6. For all vertices $d' \in L$ that received material from the previous step, set $d = d'$ and go to Step 4. Repeat until the full supply chain graph $G^{TS}\left(L, O_{l,l'}^{mat}\right)$ has been simulated.
7. If the production schedule for any mine $l_m \in L_m$ has changed, go to Step 1 to re-simulate the supply chain.

2.2 Model for global asset optimization under uncertainty

2.2.1 Generalized model

As stated in Section 2.1.3, the fundamental concept behind the simulation-optimization framework is to optimize the production scheduling variables $x_{i,t}$, along with the supply chain optimization variables, which are comprised of the destination policies $z_d^t\left(clus_{mat,n}^l\right)$ and the processing stream proportions $y_{d'}^{t,s}(mat_{l_d})$. The objective is to generate a (possibly multi-mine) production schedule that provides the optimal amount of *accessible* materials in order to maximize the total value of the supply chain, while meeting operational constraints at the mines and each destination in the supply chain, and also while considering the various stochastic (uncertain) parameters that influence the total value. The proposed mixed integer non-linear stochastic formulation is defined as follows:

Objective:

$$\max \underbrace{\sum_{l \in L_{init}} \sum_{t \in P_l} \sum_{m \in Mat_l} \sum_{r_{mat} \in R_{mat_l}} E\left\{c_{r_{mat}}^t \times \left(v_{r_{mat}}^{t,s}\right)\right\}}_{\text{(1) First stage decisions}} + \underbrace{\sum_{l \in L \setminus L_{init}} \sum_{t \in P_l} \sum_{m \in Mat_l} \sum_{r_{mat} \in R_{mat_l}} E\left\{c_{r_{mat}}^t \times \left(v_{r_{mat}}^{t,s}\right)\right\}}_{\text{(2) Recourse decisions}}$$

$$- \underbrace{\sum_{l \in L} \sum_{t \in P_l} \sum_{m \in Mat_l} \sum_{r_{mat} \in R_{mat_l}} E\left\{\overline{d_{r_{mat}}^t} \times \left(\overline{a_{r_{mat}}^t}\right)^{p(\overline{a}(r_{mat}))} + \underline{d_{r_{mat}}^t} \times \left(\underline{a_{r_{mat}}^t}\right)^{p(\underline{a}(r_{mat}))}\right\}}_{\text{(3) First or second stage recourse constraint penalties}} \quad (2)$$

Subject to:

Supply chain constraints:

$$v_{r_{mat}}^{t,s} - \overline{a_{r_{\max}}^{t,s}} \leq \overline{P_{r_{mat}}^t} \qquad \forall l \in L, mat \in Mat_l, r \in r_{mat}, t \in T_l, s \in S^{global} \quad (3)$$

$$v_{r_{mat}}^{t,s} + \underline{a_{r_{\max}}^{t,s}} \geq \underline{P_{r_{mat}}^t} \qquad \forall l \in L, mat \in Mat_l, r \in r_{mat}, t \in T_l, s \in S^{global} \quad (4)$$

$$\overline{a_{r_{\max}}^{t,s}}, \underline{a_{r_{\max}}^{t,s}} \geq 0 \qquad \forall l \in L, mat \in Mat_l, r \in r_{mat}, t \in T_l, s \in S^{global} \quad (5)$$

Mine operational constraints:

$$x_{i,t} \leq x_{j,t} \qquad \forall l_m \in L_m, i \in \{1, \ldots, N_{l_m}\}, j \in P(i), t \in \{1, \ldots, T_{l_m}\} \quad (6)$$

$$\sum_{t=1}^{T_{l_m}} x_{i,t} \leq 1 \qquad \forall l_m \in L_m, i \in \{1, \ldots, N_{l_m}\} \quad (7)$$

where:

- $E\{\bullet\}$ denotes the expectation of the contents of the braces, $\bullet$, over all simulations $s \in \{1, \ldots, S^{total}\}$.
- $L_{init} \subseteq L_d$ are the initial destinations that are fed directly from the mine; these destinations do not receive any material through the processing stream variables.
- $v_{r_{mat}}^{t,s}$ is the value of the property r_{mat} in period t and simulation s.
- $\overline{a_{r_{\max}}^{t,s}}$ is the deviation from a maximum bound $\overline{P_{r_{mat}}^{t}}$ for property r_{mat} in period t and simulation s.
- $\underline{a_{r_{\max}}^{t,s}}$ is the deviation from a minimum bound $\underline{P_{r_{mat}}^{t}}$ for property r_{mat} in period t and simulation s.
- $c_{r_{mat}}^{t} = \frac{j(r_{mat})}{(1+d(r_{mat}))^t}$ is an adjustment factor associated with property r_{mat} in period t. $j(r_{mat})$ is a constant value (e.g. 1 or -1) and $d(r_{mat})$ is a discount rate expressed as a decimal. For example, if $v_{r_{mat}}^{t,s}$ represented the undiscounted value of a metal processed and sold, $c_{r_{mat}}^{t}$ could be used to convert the property to a discounted cash flow. A negative $c_{r_{mat}}^{t}$ may be associated with a cost in the model, such as processing, mining and re-handling costs.
- $\overline{d_{r_{mat}}^{t}} = \frac{\overline{dev(r_{mat})}}{\left(1+d\left(\overline{dev(r_{mat})}\right)\right)^t} \geq 0$ and $\underline{d_{r_{mat}}^{t}} = \frac{\underline{dev(r_{mat})}}{\left(1+d\left(\underline{dev(r_{mat})}\right)\right)^t} \geq 0$are penalty costs associated with deviation variables $\overline{a_{r_{\max}}^{t,s}}$ and $\underline{a_{r_{\max}}^{t,s}}$, respectively. $\overline{dev\,(r_{mat})}$ and $\underline{dev\,(r_{mat})}$ are used to weight the constraint deviations (i.e. some constraints might be more important to adhere to than others). $d\left(\overline{dev\,(r_{mat})}\right)$ and $d\left(\underline{dev\,(r_{mat})}\right)$ are discount rates that can be used if necessary to relax the penalty associated with a constraint violation over time; this is commonly seen when applying a geological discount rate (Ramazan and Dimitrakopoulos, 2004).
- $p\left(\overline{a}\,(r_{mat})\right)$ and $p\left(\underline{a}\,(r_{mat})\right)$ are exponents associated with the upper and lower deviation variables, respectively. These can be used to severely penalize large deviations, but gradually reduce the weight of these penalties in the objective function as the optimizer finds a more feasible solution.
- $P(i)$ is used to describe the set of blocks in a mine that must be extracted in order to safely extract block i, which is often referred to as slope or precedence constraints.

It is noted that the key decision variables ($x_{i,t}$, $z_d^t\left(clus_{mat,n}^l\right)$ and $y_{d'}^{t,s}\left(mat_{l_d}\right)$) are not explicitly included in the optimization formulation presented in Eqs. (2)–(7). This is done intentionally to highlight the generality and flexibility of the formulations. Given that no two mining supply chains are alike, a modeller will need to put emphasis on different components or constraints in the supply chain. Again, it must be noted that the property values $v_{r_{mat}}^{t,s}$ are linear or non-linear functions of the key decision variables, and are obtained after simulating the supply chain. Of course, if one wishes, this formulation can be explicitly written for a given case study, including the various non-linear transformations. An example of an explicit formulation is written formally for the case study presented in Section 3.

In order to highlight some key aspects of the optimization model, the objective function presented in Eq. (2) has been decomposed into three components. The first component, (1), relates to the properties that are functions solely of the first-stage decision variables, specifically the production scheduling decisions $x_{i,t}$ and the destination policies $z_d^t\left(clus_{mat,n}^l\right)$. Some examples of this might be to subtract mining costs, stockpiling costs or treatment charges at the initial destinations in the supply chain. Note that while these calculated costs may vary between simulations, they are only dependent on the first-stage policies. The second component, (2), of the objective function relates to the properties in the supply chain that are a function of the first-stage decision variables (extraction and destination policies), along with the recourse variables – specifically, the processing stream variables $y_{d'}^{t,s}\left(mat_{l_d}\right)$. If the supply chain is complex, this might be the economic value of the metal that is sent to various customers. The third component of the objective function is used to describe penalties associated with constraint violations anywhere along the supply chain; these constraints can either be dependent solely on the first-stage decisions, or both first- and second-stage decisions, depending on where in the supply chain the constraint is applied. Some examples of constraints that may be included are mining capacity constraints (first-stage constraint violations), or much more complex constraints such as throughput capacities, total capacities, and grade blending (first-

or second-stage depending on the complexity supply chain model). It isn't, however, generally necessary to make the distinction between first-stage and second-stage properties when modelling; the only information that one might glean from this information is when there is a shortfall or surplus of desirable material in the supply chain, and when a second-stage variable is used to rectify the problem (e.g. a mill is being fed by a stockpile rather than directly from a mine).

2.2.2 Relationship to existing stochastic models

For specific configurations of supply chain models, it is possible to reduce the generalized formulation into common models that integrate geological uncertainty. For example, if one wishes to emulate the model of a basic SIP for open pit mine production scheduling (Ramazan and Dimitrakopoulos, 2012), consider a single-mine case where there are two material types defined: ore and waste. These material types have been pre-processed based on some a-priori cut-off grade policy. The supply chain graph $G^{TS}\left(L, O^{mat}_{l,l'}\right)$ simply consists of a mill and a waste dump, where the arcs in the graph only allow ore material to go the mill, and the waste material to go to the waste dump. The three components of the objective function could be designed as follows:

1. The first component would aim to maximize the NPV of the material sent to the mill, which accounts for revenues from the metal, recovery, processing costs and mining costs. These can simply be pre-processed for each block, if desired, and this property would be sent from the mine to the mill.
2. The second component of Eq. (2) would be empty because the supply chain does not contain intermediate or subsequent destinations.
3. Subtract the deviations from mine extraction capacities, processing capacities and grade blending constraints. It is possible to include geological risk discounting to defer riskier blocks to later periods.

Note that this type of model effectively eliminates the destination policy variables, $z^t_d\left(clus^l_{mat,n}\right)$, because the ore and waste policies are specified a-priori. Naturally, the entire purpose of the global asset optimizer is to enable the optimizer to make these decisions dynamically.

2.3 Algorithmic optimization with metaheuristics

Given that a supply chain model will often require the use of non-linear transformations, the generalized global asset optimization formulation can be extremely complex and very challenging to solve using conventional mathematical programming methods. For this reason, the simulation-optimization framework proposed has been designed for optimization with metaheuristics. Recall that a simulation-optimization framework is a tool that permits the dynamic evaluation of a mining complex or supply chain according to a set of prescribed variables (production schedules, destination policies and processing stream variables). An optimization method is simultaneously used to modify the variables in order to improve the quality of the solution, which is defined by the value of the objective function. Metaheuristics are generalized optimization algorithms that are particularly useful in simulation-optimization frameworks because they do not require linear formulations or any special structure in the optimization problem. Metaheuristics do not, however, guarantee a mathematically optimal solution, however have been shown in the past to give useful solutions for mining-related problems (Godoy, 2003; Montiel and Dimitrakopoulos, 2012; Goodfellow and Dimitrakopoulos, 2013).

The proposed simulation-optimization framework uses a hybrid of particle swarm optimization (PSO) and a modified simulated annealing algorithm, which will herein be referred to as multi-neighbourhood simulated annealing (MNSA). The purpose of using a combination of two metaheuristics is to overcome some of the limitations inherent in the individual method: PSO cannot be easily adapted to make production scheduling decisions without specific assumptions on block destinations, and simulated annealing-based methods cannot easily accommodate continuous variables, which is required to optimize the processing streams. Moreover, the use of two complementary metaheuristics is useful to help ensure that solutions do not get trapped in a local optimum. For the proposed framework, PSO is used to optimize the supply chain decisions, specifically the destination policies and processing stream decisions (Goodfellow and Dimitrakopoulos, 2012), and MNSA is used to help optimize the discrete (binary) decisions, specifically the destination policies and production

scheduling simultaneously. The two methods are used interchangeably during the algorithm to improve the solution and to move a solution out of a local optimum. The specifics of each of the methods are described in the subsequent sections.

2.3.1 Solution encoding scheme

The simulation-optimization framework dependent on three variables: the production scheduling decisions $x_{i,t}$, along with the supply chain optimization variables $z_d^t\left(clus_{mat,n}^l\right)$ and $y_{d'}^{t,s}\left(mat_{l_d}\right)$. It is often useful to encode these decision variables to ensure that they are compatible with a given metaheuristic; for a well-designed encoding scheme, it is possible enforce certain constraints that should never be violated during the runtime of the algorithm (e.g. slope constraints, reserve constraints and mass balancing). The solution encoding scheme for production scheduling for use with MNSA is fairly straightforward, where each block is represented on a three-dimensional grid and contains the period that the block is mined in, or a null value is it is not extracted. Of course, if the mine is extremely large, this method uses excessive memory, and the model can be condensed into a single dimensional structure. This structure permits the optimizer to quickly verify slope constraints when proposing a change in the solution. The supply chain optimization variables are encoded separately for use with the particle swarm optimization algorithm. Consider a one-dimensional solution vector, Sol, of size

$$Size\left(Sol\right) = \underbrace{\sum_{l\in L_m}\sum_{t\in T_l}\sum_{mat\in O_l} n_{clusters}^{l,mat}}_{\text{Destination policies}} + \underbrace{\sum_{l\in L_d}\sum_{t\in T_l}\sum_{mat\in O_l}\sum_{d\in D(mat)}\sum_{s\in\{1,\ldots,S^{Total}\}} 1}_{\text{Processing streams}} \tag{8}$$

where O_l is used to define the set of output materials at a location $l \in L$ in the supply chain. The first component of the solution vector is used to define the destination policy for each cluster in a given material type, in each period and for each mine. Each destination is given a unique identifier, however an encoding scheme is used to convert the destination identifier to a discrete variable, bounded by $[0, N\left(D\left(mat\right)\right)]$, where $N\left(D\left(mat\right)\right)$ is used to denote the total number of candidate destinations for material mat. This encoding is necessary for the particle swarm optimization algorithm, which prefers to operate in a continuous space without jump discontinuities, which would likely happen if the destination identifiers were used directly in the encoding scheme. A decoding scheme that converts the encoded variable to a destination identifier is stored in a compact table. The second component of Eq. (8) relates to the processing stream (recourse) variables, $y_{d'}^{t,s}\left(mat_{l_d}\right)$. Each destination in the supply chain graph $G^{TS}\left(L, O_{l,l'}^{mat}\right)$ that has an output material has a recourse variable for each candidate destination and simulation. When using the metaheuristics, it is necessary to enforce the material flow conditions (cannot send out more material than is available). In order to satisfy this, when the sum of the outflow is greater than one, i.e. $\sum_{d'\in D_{mat_d}} y_{d'}^{t,s}\left(mat_d\right) > 1$, the $y_{d'}^{t,s}\left(mat_{l_d}\right)$ variables are normalized as follows:

$$y_{d'}^{t,s}\left(mat_{l_d}\right) = \frac{y_{d'}^{t,s}\left(mat_{l_d}\right)}{\sum_{d'\in D_{mat_d}} y_{d'}^{t,s}\left(mat_d\right)} \tag{9}$$

2.3.2 Supply chain optimization with particle swarm optimization

Particle swarm optimization (Kennedy and Eberhart, 1995) is a population-based metaheuristic that is capable of optimizing over both discrete and continuous variables, making it particularly suitable for optimizing the supply chain. The goal of the algorithm is to find a global minimum (or maximum) in a multi-dimensional space by initializing a swarm of particles with random solution vector positions and velocities. As the particles explore the domain, the swarm of particles converges on a global optimum. Consider a set of N_p particles, where each particle is represented by its own distinct supply chain optimization solution vector, Sol. Each particle $p \in N_p$ has three vectors: the current solution at iteration t, $x^p\left(t\right)$, the particle's best solution vector, $x^{p,best}$, and a velocity vector for a given iteration t, $v^p\left(t\right)$, each of length $Size\left(Sol\right)$. Additionally, consider the solution vector of the particle that has the best objective function found during the algorithm, x^{global}. At iteration $t+1$ in the algorithm, a particle's velocity is updated as follows:

$$v^p\left(t+1\right) = c_1 v^p\left(t\right) + \left(c_2 \times rand() \times \left(x^{p,best} - x^p\right)\right) + \left(c_3 \times rand() \times \left(x^{global} - x^p\right)\right) \tag{10}$$

where $v^p(t+1)$ is particle p's new velocity in iteration $t+1$, c_1 gives weight to the particle's previous velocity, c_2 gives weight to the difference between the particle's current solution and its best solution, c_2 gives weight to the difference between the particle's current solution and the global best solution found by iteration t and $rand() \in [0,1]$ is a uniform random number. The particle's velocity is therefore a function of its inertia and also an attraction towards previously found solutions with a better objective function. The particle's solution vector for iteration $t+1$ is then updated as follows:

$$x^p(t+1) = x^p(t) + v^p(t+1) \tag{11}$$

It is noted that if any element of the solution vector $x^p(t+1)$ exceeds the bounds $[0, N(D(mat))]$ of the encoded solution vector from Section 2.3.1, the element will be set to the nearest bound. This is used to ensure that the cluster of material can only be sent to a feasible destination.

After the particle's solution vector has been updated, the supply chain is then evaluated or simulated (Section 2.1.3) to compute the objective function defined in Eq. (2). Let $f(x^p(t))$, $f\left(x^{p,best}\right)$ and $f\left(x^{global}\right)$ represent the simulated objective function value for the particle's current solution vector, the particle's best solution vector and the global best solution vector, respectively, found at iteration t, and are calculated from Eq. (2). Given that the objective function in Eq. (2) is defined as a maximization function, if $f(x^p(t)) \geq f\left(x^{p,best}\right)$, then the particle's best solution vector is updated, i.e. $x^{p,best} = x^p$. If $f\left(x^{p,best}\right) \geq f\left(x^{global}\right)$, then the global best solution vector is updated ($x^{global} = x^{p,best}$).

2.3.3 Production schedule and destination policy optimization with multi-neighbourhood simulated annealing

The main limitation of particle swarm optimization is that it has a tendency to converge in a sub-optimal solution for high-dimensional problems (Yanbin, 2008). Additionally, it is challenging to develop an efficient encoding or decoding scheme for use with production scheduling optimization, given that the solution must always guarantee that the slope constraints in Eq. (6) are satisfied. To overcome these challenges, an adapted version of the simulated annealing metaheuristic (Kirkpatrick et al., 1983; Geman and Geman, 1984) is used. Simulated annealing works well with discrete variables, and has been successfully applied for several mine design optimization problems (Godoy, 2003; Montiel and Dimitrakopoulos, 2012; Goodfellow and Dimitrakopoulos, 2013). This metaheuristic is applied intermittently to the global best solution vector, x^{global}, found by the particle swarm supply chain optimizer, as discussed in Section 2.3.2.

For the proposed simulation-optimization framework, the modified simulated annealing algorithm attempts to perturb a production schedule ($x_{i,t}$) and destination policies ($z_d^t\left(clus_{mat,n}^l\right)$) to move the global asset optimizer out of a local optimum. Any attempted change in solution, be it production schedule or destination policy, is referred to as a perturbation. A set of candidate perturbations that are possible for a given solution vector is referred to as a neighbourhood. A perturbation in the production schedule can be found by randomly selecting a block from a mine and attempting to extract it in a different production period. In order to ensure slope stability, the algorithm does a depth-first search (Cormen et al., 2009) to explore the block's overlying or underlying blocks (Khalokakaie et al., 2000) and attempts to also move them to a new period. For a more detailed review of simulated annealing for mine designs, the reader is referred to Goodfellow and Dimitrakopoulos (2013).

Simulated annealing is a metaheuristic modelled after the metallurgical phenomenon of cooling a metal slowly to increase the size of the crystals and minimize the number of defects. At the beginning of the algorithm, the optimizer automatically accepts a perturbation of the solution if it yields a better objective function value, however it is also permitted to accept sub-optimal perturbations in order to avoid being trapped in a local optimum. As the algorithm progresses, the number of sub-optimal perturbations that are accepted decreases, until it eventually becomes greedy (only accepts solutions with better objective functions). In the classic simulated annealing algorithm, the acceptance probability for a perturbation of the solution vector for a maximization problem is based on the following acceptance probability distribution:

$$P(f(x_{new}), f(x), T) = \begin{cases} 1 & \text{if } f(x_{new}) \geq f(x) \\ \exp\left(-\left|f(x_{new}) - f(x)\right| / T\right) & \text{otherwise} \end{cases} \tag{12}$$

where $f(x)$ and $f(x_{new})$ are the objective functions before and after a perturbation, respectively, and T is a parameter called the "annealing temperature". As the algorithm progresses, the temperature is reduced until only minor changes in the objective function are accepted; this is often controlled by the initial temperature at the start of the algorithm, $T(0)$, and the cooling schedule, which is defined by a reduction factor, $k \in [0, 1]$, and a number of iterations before the reduction factor is applied, n_{iter}.

One of the primary difficulties of the simulated annealing algorithm is the calibration of the initial temperature; naturally, this parameter is dependent on the magnitude of change in objective function that any given perturbation will have. This parameter is particularly problematic for simulated annealing with multiple neighbourhoods or variables, such as the case in the proposed method where both production scheduling moves and destination policies are made, because the different neighbourhoods for a set of variables may have different effects on the change in objective function value. Figure 1 shows an example of the cumulative distributions of the difference between objective function values for sub-optimal candidate perturbations for the production scheduling and destination policy neighbourhoods, i.e. perturbations where $f(x_{new}) - f(x) < 0$. The difference between the distributions of sub-optimal perturbations is drastically different; in practice, this means that for a very large annealing temperature, the optimizer will may limit the number of sub-optimal changes in production schedule, but will likely accept all destination policy changes. As the temperature decreases, the optimizer is more likely to only accept sub-optimal destination policy changes, and reject all sub-optimal production schedule changes. The classical simulated annealing method with a single temperature ignores the inherent relationship between the two decision variables and neighbourhoods. For this reason, a multi-neighbourhood simulated annealing (MNSA) is proposed.

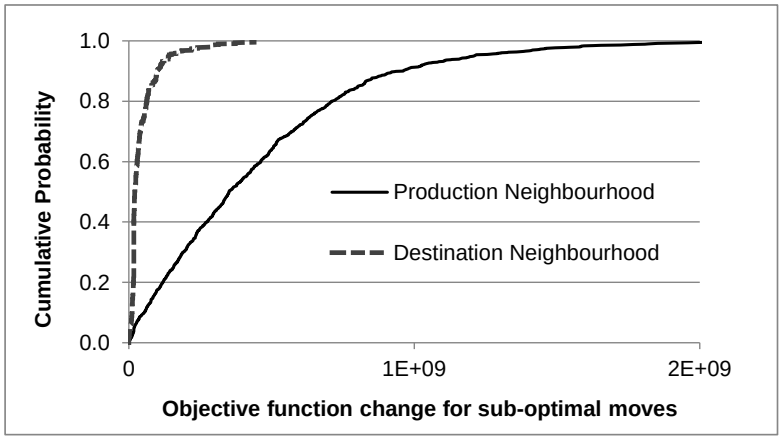

Figure 1: Example of cumulative probability distributions of objective function changes for sub-optimal perturbations of two neighbourhoods.

In MNSA, the cumulative probability distributions of objective function changes for sub-optimal perturbations are first constructed for each neighbourhood by proposing random perturbations. Rather than using a fixed temperature, T, for both neighbourhoods in Eq. (12), the optimizer uses two temperature variables T_{prod} and T_{dest} for the production schedule and destination policy neighbourhoods, respectively, which are in turn controlled by a single cumulative distribution probability ρ. For a fixed ρ, the respective temperature variables (T_{prod} and T_{dest}) are found from the cumulative probability plots (Figure 1). The cooling schedule (k,n_{iter}) is then applied directly to ρ, which in turn relates to increasingly small T_{prod} and T_{dest} temperatures. As the algorithm progresses, the information garnered from any new proposed sub-optimal perturbations is used as feedback to update the cumulative distributions; this better reflects the current search space, rather than the search space when the MNSA commenced.

As stated previously, the PSO and MNSA algorithms are used interchangeably for both local improvement and to avoid getting stuck in a local optimum. For blending problems or problems with complex supply chains, PSO is extremely useful for refining and improving the supply chain, and MNSA is useful to move away from local optima. For simple cases where there are not any intermediate or subsequent destinations, such as the

case study in Section 3, MNSA is primarily used and PSO is used to refine the solutions. The software used for the proposed methodology permits changing which algorithm (PSO or MNSA) is used dynamically, thus being able to switch between the two methods when needed. Future work will focus on a generalized algorithm that selects the appropriate metaheuristic when needed in order to give a more automated approach.

3 Case Study – Application at a Copper-Gold Deposit

The proposed global asset optimization framework is demonstrated on a copper-gold mining complex, which is loosely based off a real-world deposit, but has been modified substantially for the sake of both confidentiality and discussion.

3.1 Overview of the mining complex

In the given case study, a single mine supplies materials to a mining complex that extracts both gold and copper. Figure 2 summarizes the definition of the mine's material types along with the various processing options. The mine is represented by a set of 50 equally probable geological simulations with variable copper, gold, tonnages and material types; 40 of the simulations are used for optimization and the remaining 10 are used to verify the robustness of the stochastic solution. The mine is comprised of three main material groups: sulphides, transition and oxides. Each of these major groups is separated into two material types for use with the proposed methodology (Figure 2). In order to model the material flows in the processing paths, the sulphide and transition material groups are both separated into two different material types based on being above or below 0.2% copper in order to be compatible with the heap leach chemistry requirements. The oxide materials are automatically classified based on potential ore and waste; the waste group is material below the marginal cut-off grade of the process or is material that is not simulated, thus automatically considered as waste.

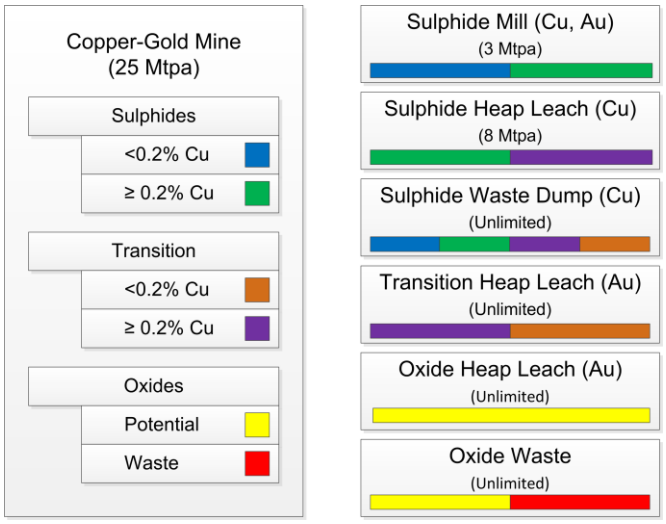

Figure 2: Definition of material types at the copper-gold mine, along with the various destinations. Note that the input materials at the destinations have been colour-coded according to the materials in the mine.

The model's destinations consist of a sulphide mill (SM), a sulphide heap leach (SHL), a sulphide dump leach (SDL), a transition heap leach (THL), an oxide heap leach (OHL) and an oxide waste dump. The sulphide mill, which is limited to processing three million tonnes per year, only accepts sulphide materials and produces both copper and gold as products. The sulphide heap leach has an eight million tonnes per year capacity for both sulphide and transition materials, however, for chemistry reasons, it can only process the materials above 0.2% copper, hence the creation of distinct material types around this grade. The sulphide waste dump is essentially a waste dump where excess sulphide and transition materials go for leaching,

regardless of whether or not it is profitable to treat the material. Both of the sulphide leach processes extract only copper as a product. The transition and oxide heap leaches accept only transition or oxide materials, respectively, and both extract only gold. The oxide waste dump accepts both oxide materials, however does not treat any of the material. All leaching processes, excluding the SHL, are assumed to have unlimited capacity.

With the exception of the oxide waste dump, all destinations have variable grade-recovery curves that are based on the average grade of the incoming material at a process in a given period. These grade-recovery curves are shown in Figure 3 and are expressed relative to the process with the highest recovery for confidentiality purposes. As a result of the dynamic recoveries, the oxide materials are not explicitly classified as ore or waste, given that it may be desirable to not treat the "potential" oxide material if the average gold grade in a given year is low, which might be related to an uneconomical recovery. The non-linear grade-recoveries also have interesting implications when considering the transition material: for a given block or cluster that has (hypothetically) similar copper and gold economic values, the selected destination would be the one that profits the most from an increase in average grade, hence increased recovery after processing costs are considered. As a result, one cannot assume that block destinations can be specified a-priori in a greedy manner because it is the recovery of the aggregated material sent to a given process that determines the potential value.

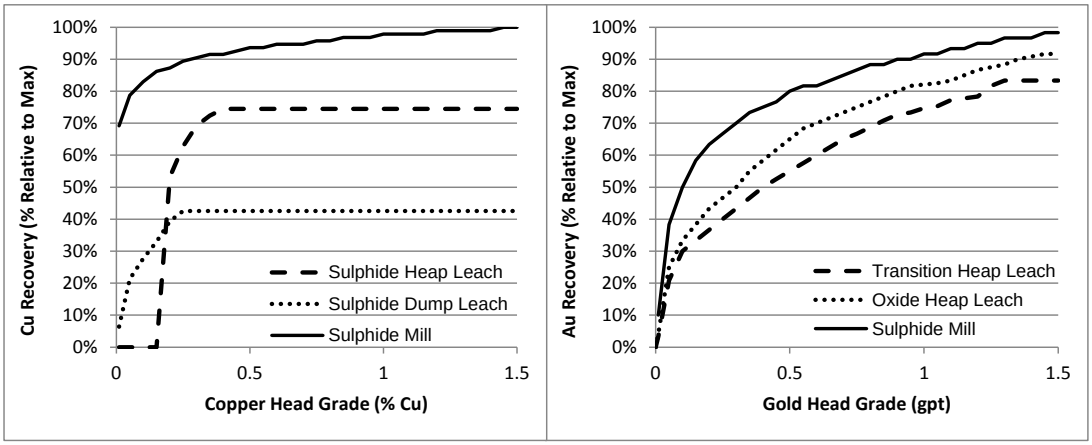

Figure 3: Copper (left) and gold (right) grade-recovery curves for the various processes. Note that the recoveries are expressed relative to the process with the maximum recovery.

Table 1 shows a summary of the mining, processing and economic parameters used in the optimization models. It must be noted that for confidentiality purposes, the mining and processing costs are expressed relative to a base cost "x" to give an idea about the order of magnitude of costs for the various processes. It can be seen that despite the fact that the sulphide mill has the highest recoveries for both copper and gold, the processing cost is substantially higher than the destinations that process only one element.

3.2 Stochastic optimization model

The proposed optimization model seeks to maximize the net present value of the mining complex while minimizing deviations from the mining capacity and processing capacities of the sulphide mill and the sulphide heap leach. It has been seen through testing with conventional mine planning software that these two destinations generate the vast majority of the mining complex's profits (40% and 58%, respectively), so it is desirable to control the risk of the quantities of materials going to these destinations in the mine production schedule. It is noted that the non-linearities of the model arise from the use of dynamic recovery curves, which in turn depend on the average grade of the material sent to a given destination. The definitions and explicit optimization formulation are as follows:

Table 1: Summary of mining, processing and economic parameters used. Note that all costs are expressed relative to a base cost (x) that is not disclosed.

Mining parameters	
Mining cost (relative to base cost x)	\$1.00 $*x$ /tonne
Slope angle	45°
Total number of blocks	30,098
Processing costs (relative to base cost x)	
Sulphide mill	\$11.30 $*x$ /tonne
Sulphide heap leach	\$2.98 $*x$ /tonne
Sulphide dump leach	\$1.87 $*x$ /tonne
Transition heap leach	\$2.15 $*x$ /tonne
Oxide heap leach	\$2.06 $*x$ /tonne
Economic parameters	
Copper price (including selling and G&A costs)	\$2.88 /lb Cu recovered
Gold price (including G&A costs)	\$1480 /oz Au recovered
Discount rate	7%

Definitions:

- $v_i^{btonnage}(s)$, $v_i^{cutonnage}(s)$ and $v_i^{augrams}(s)$ denote block i's total tonnage, copper tonnage and grams of gold, respectively, in simulation s.
- $mat \in \{1, \ldots, 5\}$ denote the low-grade (1) and high-grade sulphide materials (2), the low-grade (3) and high-grade (4) transition materials and potential oxide (5) materials.
- $i \in \{1, \ldots, N\}$ indexes the blocks considered for extraction, where $N = 30098$ is the number of blocks in the model.
- $s \in \{1, \ldots, 20\}$ indexes the number of geological simulations considered.
- $t \in \{1, \ldots, 22\}$ indexes the time periods considered.
- $clus_{mat,n}$ denotes the cluster of material type mat, which is indexed by n. All materials are grouped into 25 clusters, with the exception of the oxide waste, which only contains one cluster. The total number of clusters considered for each time period is therefore 126.
- $z_l^t\left(clus_{mat,n}^l\right) \in \{0, 1\}$ denotes whether or not cluster $clus_{mat,n}$ is sent to destination $l \in \{SM, SHL, SDL, THL, OHL\}$ in period t.
- $f_{metal}^l(g)$ denotes the recovery for metal $metal \in \{Cu, Au\}$ evaluated at destination $l \in \{SM, SHL, SDL, THL, OHL\}$ with average head grade g. This is evaluated using a look-up table and interpolation for the grade-recovery curves depicted in Figure 3.
- mc is the mining cost in dollars per tonne of material extracted.
- val_{Cu}, val_{Au} are the metal values for copper (per tonne) and gold (per gram), respectively.
- tc_l is the treatment (processing, leaching) cost per tonne of material the destination $l \in \{SM, SHL, SDL, THL, OHL\}$.

Objective:

$$\max \underbrace{E\{PV_{SM}\} + E\{PV_{SHL}\} + E\{PV_{SDL}\} + E\{PV_{THL}\} + E\{PV_{OHL}\} - E\{MC\}}_{\text{First-stage policies}} \\ \underbrace{- E\left\{\overline{p^{SM}}\right\} - E\{\underline{p^{SM}}\} - E\left\{\overline{p^{SHL}}\right\} - E\{\underline{p^{SHL}}\} - E\left\{\overline{p^{Mine}}\right\}}_{\text{Recourse penalties}} \quad (13)$$

Subject to:

Mining slope and reserve constraints:

$$x_{i,t} \leq x_{j,t} \qquad i \in \{1,\ldots,N\}, j \in P(i), t \in \{1,\ldots,22\} \tag{14}$$

$$\sum_{t=1}^{22} x_{i,t} \leq 1 \qquad \forall i \in \{1,\ldots,N\} \tag{15}$$

Cluster property calculations (total tonnes, copper tonnes, gold grams) for all $mat \in \{1,\ldots,5\}, n \in \{1,\ldots,25\}$, $s \in \{1,\ldots,40\}, t \in \{1,\ldots,22\}$*:*

$$v_t^{btonnage}\left(clus_{mat,n}(s)\right) = \sum_{i \in clus^l_{mat,n}(s)} v_i^{btonnage}(s) \cdot x_{i,t} \tag{16}$$

$$v_t^{cutonnage}\left(clus_{mat,n}(s)\right) = \sum_{i \in clus^l_{mat,n}(s)} v_i^{cutonnage}(s) \cdot x_{i,t} \tag{17}$$

$$v_t^{augrams}\left(clus_{mat,n}(s)\right) = \sum_{i \in clus^l_{mat,n}(s)} v_i^{augrams}(s) \cdot x_{i,t} \tag{18}$$

Quantities of material received at the destinations for all $s \in \{1,\ldots,40\}, t \in \{1,\ldots,22\}$*:*

$$v_t^{SMTonnage}(s) = \sum_{mat\in\{1,2\}} \sum_{n=1}^{25} v_t^{btonnage}\left(clus_{mat,n}(s)\right) \times z_{SM}^t\left(clus^l_{mat,n}\right) \tag{19}$$

$$v_t^{SMCuT}(s) = \sum_{mat\in\{1,2\}} \sum_{n=1}^{25} v_t^{cutonnage}\left(clus_{mat,n}(s)\right) \times z_{SM}^t\left(clus^l_{mat,n}\right) \tag{20}$$

$$v_t^{SMAuG}(s) = \sum_{mat\in\{1,2\}} \sum_{n=1}^{25} v_t^{augrams}\left(clus_{mat,n}(s)\right) \times z_{SM}^t\left(clus^l_{mat,n}\right) \tag{21}$$

$$v_t^{SHLTonnage}(s) = \sum_{mat\in\{2,4\}} \sum_{n=1}^{25} v_t^{btonnage}\left(clus_{mat,n}(s)\right) \times z_{SHL}^t\left(clus^l_{mat,n}\right) \tag{22}$$

$$v_t^{SHLCuT}(s) = \sum_{mat\in\{2,4\}} \sum_{n=1}^{25} v_t^{cutonnage}\left(clus_{mat,n}(s)\right) \times z_{SHL}^t\left(clus^l_{mat,n}\right) \tag{23}$$

$$v_t^{SDLTonnage}(s) = \sum_{mat\in\{1,2,3,4\}} \sum_{n=1}^{25} v_t^{btonnage}\left(clus_{mat,n}(s)\right) \times z_{SDL}^t\left(clus^l_{mat,n}\right) \tag{24}$$

$$v_t^{SDLCuT}(s) = \sum_{mat\in\{1,2,3,4\}} \sum_{n=1}^{25} v_t^{cutonnage}\left(clus_{mat,n}(s)\right) \times z_{SDL}^t\left(clus^l_{mat,n}\right) \tag{25}$$

$$v_t^{THLTonnage}(s) = \sum_{mat\in\{3,4\}} \sum_{n=1}^{25} v_t^{btonnage}\left(clus_{mat,n}(s)\right) \times z_{THL}^t\left(clus^l_{mat,n}\right) \tag{26}$$

$$v_t^{THLAuG}(s) = \sum_{mat\in\{3,4\}} \sum_{n=1}^{25} v_t^{augrams}\left(clus_{mat,n}(s)\right) \times z_{THL}^t\left(clus^l_{mat,n}\right) \tag{27}$$

$$v_t^{OHLTonnage}(s) = \sum_{n=1}^{25} v_t^{btonnage}\left(clus_{mat,n}(s)\right) \times z_{OHL}^t\left(clus^l_{mat,n}\right) \tag{28}$$

$$v_t^{OHLAuG}(s) = \sum_{n=1}^{25} v_t^{augrams}\left(clus_{5,n}(s)\right) \times z_{OHL}^t\left(clus^l_{5,n}\right) \tag{29}$$

Metal recoveries as functions of grade-recovery curves shown in Figure 3 for all $s \in \{1,\ldots,40\}, t \in \{1,\ldots,22\}$*:*

$$v_t^{SMCu\mathrm{Rec}}(s) = f_{Cu}^{SM}\left(v_t^{SMCuT}(s)/v_t^{SMTonnage}(s)\right) \tag{30}$$

$$v_t^{SMAu\mathrm{Rec}}(s) = f_{Au}^{SM}\left(v_t^{SMAuG}(s)/v_t^{SMTonnage}(s)\right) \tag{31}$$

$$v_t^{SHLCu\mathrm{Rec}}(s) = f_{Cu}^{SHL}\left(v_t^{SHLCuT}(s)/v_t^{SHLTonnage}(s)\right) \tag{32}$$

$$v_t^{SDLCu\mathrm{Rec}}(s) = f_{Cu}^{SDL}\left(v_t^{SDLCuT}(s)/v_t^{SDLTonnage}(s)\right) \tag{33}$$

$$v_t^{THLAu\mathrm{Rec}}(s) = f_{Au}^{THL}\left(v_t^{THLAuG}(s)/v_t^{THLTonnage}(s)\right) \tag{34}$$

$$v_t^{OHLAu\mathrm{Rec}}(s) = f_{Au}^{OHL}\left(v_t^{OHLAuG}(s)/v_t^{OHLTonnage}(s)\right) \tag{35}$$

Expected net present values for the various destinations:

$$\begin{aligned} E\{PV_{SM}\} = {} & \frac{1}{40}\sum_{s=1}^{40}\sum_{t=1}^{22}\frac{1}{1.07^t}\left(v_t^{SMCuT}(s)\times v_t^{SMCu\mathrm{Rec}}(s)\times val_{Cu} - v_t^{SMTonnage}(s)\times tc_{SM}\right) \\ & + \frac{1}{40}\sum_{s=1}^{20}\sum_{t=1}^{22}\frac{1}{1.07^t}\left(v_t^{SMAuG}(s)\times v_t^{SMAu\mathrm{Rec}}(s)\times val_{Au}\right) \end{aligned} \tag{36}$$

$$E\{PV_{SHL}\} = \frac{1}{40}\sum_{s=1}^{40}\sum_{t=1}^{22}\frac{1}{1.07^t}\left(v_t^{SHLCuT}(s)\times v_t^{SHLCu\mathrm{Rec}}(s)\times val_{Cu} - v_t^{SHLTonnage}(s)\times tc_{SHL}\right) \tag{37}$$

$$E\{PV_{SDL}\} = \frac{1}{40}\sum_{s=1}^{40}\sum_{t=1}^{22}\frac{1}{1.07^t}\left(v_t^{SDLCuT}(s)\times v_t^{SDLCu\mathrm{Rec}}(s)\times val_{Cu} - v_t^{SDLTonnage}(s)\times tc_{SDL}\right) \tag{38}$$

$$E\{PV_{THL}\} = \frac{1}{40}\sum_{s=1}^{40}\sum_{t=1}^{22}\frac{1}{1.07^t}\left(v_t^{THLAuG}(s)\times v_t^{THLAu\mathrm{Rec}}(s)\times val_{Au} - v_t^{THLTonnage}(s)\times tc_{THL}\right) \tag{39}$$

$$E\{PV_{OHL}\} = \frac{1}{40}\sum_{s=1}^{40}\sum_{t=1}^{22}\frac{1}{1.07^t}\left(v_t^{OHLAuG}(s)\times v_t^{OHLAu\mathrm{Rec}}(s)\times val_{Au} - v_t^{OHLTonnage}(s)\times tc_{OHL}\right) \tag{40}$$

Mining cost:

$$E\{MC\} = \frac{1}{40}\sum_{s=1}^{40}\sum_{t=1}^{22}\frac{1}{1.07^t}\left(\sum_{i=1}^{N} v_i^{btonnage}(s)\cdot x_{i,t} * mc\right) \tag{41}$$

Constraint deviation penalties:

$$E\left\{\overline{p^{SM}}\right\} = \frac{1}{40}\sum_{s=1}^{40}\sum_{t=1}^{10}\frac{25}{1.1^t}\left(\max\left\{0, v_t^{SMTonnage}(s) - 3000000\right\}\right)^{1.05} \tag{42}$$

$$E\left\{\underline{p^{SM}}\right\} = \frac{1}{40}\sum_{s=1}^{40}\sum_{t=1}^{10}\frac{25}{1.1^t}\left(\max\left\{0, 2900000 - v_t^{SMTonnage}(s)\right\}\right)^{1.05} \tag{43}$$

$$E\left\{\overline{p^{SHL}}\right\} = \frac{1}{40}\sum_{s=1}^{24}\sum_{t=1}^{22}\frac{10}{1.1^t}\left(\max\left\{0, v_t^{SHLTonnage}(s) - 8000000\right\}\right)^{1.05} \tag{44}$$

$$E\left\{\underline{p^{SHL}}\right\} = \frac{1}{40}\sum_{s=1}^{40}\sum_{t=1}^{22}\frac{10}{1.1^t}\left(\max\left\{0, 7800000 - v_t^{SHLTonnage}(s)\right\}\right)^{1.05} \tag{45}$$

$$E\left\{\overline{p^{Mine}}\right\} = \frac{1}{40}\sum_{s=1}^{40}\sum_{t=1}^{10}10\times\left(\max\left\{0, \sum_{i=1}^{N} v_i^{btonnage}(s)\cdot x_{i,t} - 25000000\right\}\right) \tag{46}$$

As stated previously, the objective function (Eq. (13)) attempts to maximize the net present value of the metals processed over the life of the mining complex. The slope (precedence) constraints are enforced through Eq. (14) and Eq. (15) is used to ensure that a block is only set for extraction at most once. Equations (16)–(18) are used to aggregate the values of the properties of the blocks extracted into their respective clusters, which relates to the first step of the supply chain simulation algorithm. It is noted that these equations are dependent on the block extraction (production scheduling) decisions, $x_{i,t}$. Equations (19)–(29) are used to calculate the quantities of metal and total tonnages sent from the mine to their assigned destinations, which are defined according to the destination policy variable $z_l^t\left(clus_{mat,n}^l\right)$. Equations (30)–(35) are used to describe the calculation of the recovery based on evaluating the appropriate grade-recovery curve; it is noted that the grade of the metal is the average grade of the material received in a given period and simulation. Equations (36)–(40) are used to calculate the expected present value (PV) at the destinations; recall that 40 equally probable geological simulations are used in the optimization process, hence the expected value is calculated by averaging over the 40 simulations. Equation (41) is used to calculate the PV of the mining costs, which is a function of all material extracted over the life of the mine. Equations (42) and (43) are used to penalize the objective function for deviations at the sulphide mill during the first 10 years, whereby the penalty cost is \$25/tonne of deviation. It is noted that Eq. (43) is used to help guide the optimizer to have a risk profile distributed around the sulphide mill's capacity of 3Mtpa; by not properly calibrating the penalty cost and not including Eq. (43), the optimizer may seek a risk-averse solution whereby there is no chance of filling the process up to its capacity. Equations (44) and (45) are used to control the risk profiles of the tonnages at the sulphide heap leach, where the penalty cost is set to \$10/tonne of deviation. It is noted that Eq's. (42)–(45) all use geological risk discounting (10%) and an exponent for the penalty (1.05) in an attempt to better control the risk profiles over the life of the mining complex. Finally, Eq. (46) is used to control deviations from the mine extraction capacity of 25Mtpa; for this constraint, geological risk discounting and penalty exponents are not used.

3.3 Numerical results

An initial production schedule is first generated for an estimated (deterministic) orebody model using Gemcom Whittle (Whittle, 2007; Whittle, 2009). The estimated orebody model has been generated by averaging the grades in the given simulations and re-classifying the material types in the same manner that the simulations are classified. Whittle generates a bench-wise long-term production schedule, and the resulting sequence has been re-optimized with the proposed framework to correct any slope constraint violations that are a result of fractional benches. All clustering parameters used for both the deterministic and stochastic cases are listed in Table 2. Whittle indicates a 0.42% improvement in cumulative net present value (NPV) over the proposed method, however this difference is minor and is mostly caused by difference in methodology used; Whittle can obtain fractional solutions for a given bench (i.e. fractional solution for an aggregate of blocks that are spatially contiguous), whereas the proposed methodology uses binary decision variables for destination policies for aggregates of blocks. An interesting prospect for future research would be to refine the aggregations used for destination policies through the use of metaheuristic clustering (Das et al., 2009), which would likely improve the quality of clusterings and increase the NPV.

Table 2: Summary of clustering parameters used in the case study.

Material	Number of Clusters	Clustering Properties
Sulphide (1) < 0.2% Cu	25	Cu, Au
Sulphide (2) = 0.2% Cu	25	Cu, Au
Transition (3) < 0.2% Cu	25	Cu
Transition (4) = 0.2% Cu	25	Cu, Au
Oxide potential	25	Au
Oxide waste	1	N/A

Using the schedule generated from the deterministic model optimized with the proposed method, it is possible obtain a risk analysis by fixing the production schedule and generating destination policies that are robust under uncertainty, i.e. optimize the supply chain only (Goodfellow and Dimitrakopoulos, 2012).

Figure 4 shows a comparison between the tonnage and NPV risk profiles for the optimized supply chain considering uncertainty and the purely deterministic case. It is noted that the true NPV values are withheld for confidentiality purposes, and are expressed relative to the cumulative NPV of the long-term production schedule from the pure deterministic case. The risk profiles are presented as the P-10, P-50 and P-90 values, i.e. the value for which 10, 50 and 90% of the simulations fall below, respectively. For the deterministic case and the associated risk profiles, the sulphide mill is filled to its maximum capacity (3 Mt) for the first 10 years, however there is not enough sulphide material to continue feeding it up to capacity for the remainder of the mine life. Additionally, during the first ten years, the risk profiles show an average of 6.4% deviations from the processing capacity of the sulphide mill. One of the major difference between the deterministic and risk profiles is that the deterministic profile shows substantially more material going to the mill than

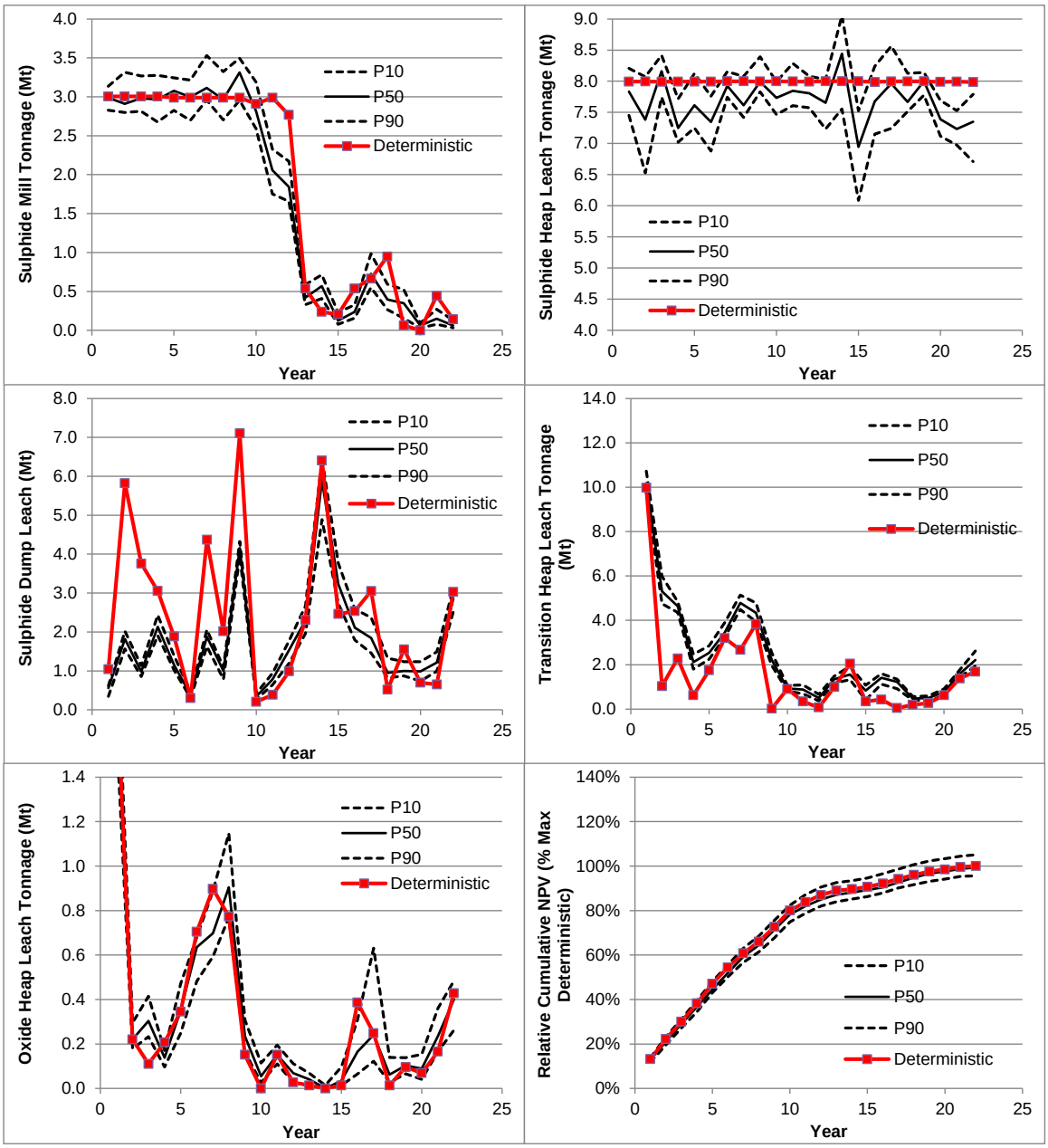

Figure 4: Comparison of risk analysis of the conventional long-term production schedule to the results of deterministic model.

the risk analysis indicates in periods 11 and 12; upon further investigation, this is due to a lack of available sulphide material. Interestingly, this does not impact the net present value of the schedule because the risk analysis has a higher head grade, hence recovery, for these two periods. The sulphide heap leach graph shows that it is used to its full capacity (8 Mt) over the life of the mining complex for the deterministic model, whereas the risk profiles indicate that the deterministic schedule doesn't have sufficient quantities to send to this process, or the material is often more valuable sent to other destinations. On average, the quantity of material sent to the sulphide heap leach is 5.2% less than the deterministic model over the life of the mine, with an average risk of 5.6% for being above or below the target capacity. Given that this destination contributes 58% to the total NPV of the mining complex for the deterministic case, this risk is substantial and could benefit from the proposed stochastic global asset optimizer. There is a drastic reduction in the quantity of material going to the sulphide dump leach at the beginning of the mine's life when comparing the deterministic solution to the stochastic solution, which is associated with an increase in tonnage at the transition heap leach process. This result is typical for risk analyses and is caused by the fact that the simulations have a different gold grade-tonnage distribution than the deterministic model; the supply chain optimizer is taking advantage of the higher-grade material that is typically smoothed out with estimated (expected value) geological models. The tonnages going to the oxide leach pad are quite similar for both the deterministic and risk profiles, which indicate that the estimated and simulated models are similar for this destination. Finally, Figure 4 also shows a risk analysis of the cumulative NPV for a deterministic schedule. Both the deterministic and the risk profiles from the simulations indicate a similar cumulative NPV, on average, despite the fact that there is a fair amount of risk in terms of quantities of material going to the sulphide mill or sulphide heap leach. This result is possible given the fact that the simulations typically have more variability for both the copper and gold distributions than the estimated (E-type, average) model; a higher variability of gold, for example, will not only relate to some higher-grade material, but also will likely yield higher recoveries at the various destinations. Given that the risk analysis indicates similar NPVs despite the risk profiles indicating a substantial shortfall of sulphide heap leach material in the deterministic schedule, using a stochastic optimizer may be able to not only improve the NPV, but increase the certainty that there is a sufficient supply of materials to fully utilize the capacities of the sulphide mill and the sulphide heap leach destinations.

The proposed stochastic global asset optimizer is tested using the model defined by Eqs. (13)–(46) using 40 geological simulations; the simulations are sequentially fed into the optimizer to avoid excessive computing times. Figure 5 shows the risk profiles (P10, P50 and P90) of the solution from the stochastic global optimizer along with the results of the deterministic solution for comparison. The solution indicates a much tighter control over the risk profiles of the sulphide mill than the deterministic solution – an average of 2.9% deviation over the first 10 years of operation. This is a substantial difference in risk when compared to the 6.4% deviations from the deterministic solution shown in Figure 4. The sulphide heap leach also shows consistent quantities of material over the life of the operation, with an average of 3.1% deviation from the target capacity of 8Mtpa. An interesting result in both graphs is that the down-side risk of not producing material to feed either the sulphide mill or sulphide heap leach is minimal (i.e. the difference between the P10 and P50 curves); this implies that the production schedule and destination policies have very little risk in terms of not providing enough material to be able to fill the destination's respective capacities for the input simulations. In fact, the optimizer has opted for a schedule that has a substantial amount of upside potential – the difference between the P90 and P10 profiles. The effects of geological risk discounting are apparent for the sulphide heap leach from years 14 to 22; the difference between the P10 and P90 profiles and the P50 profile becomes larger when comparing to the first 13 years of production. This implies the schedule is indeed attempting to leave riskier material to later in the mining complexes life when more geological information is available.

Figure 5 also shows that there is a substantial difference in sulphide dump leach and transition heap leach tonnages for the first 4 years when compared to the risk profiles from the deterministic solution. The stochastic solution opts to send more material to the sulphide dump leach, and less material to the transition heap leach; admittedly, this may be a result of the optimizer seeking to send sub-optimal material from the transition heap leach to the sulphide heap leach in order to satisfy the minimum capacity constraint in Eq. (45). One must note, however, that both the supply chain optimization for the risk analysis of the

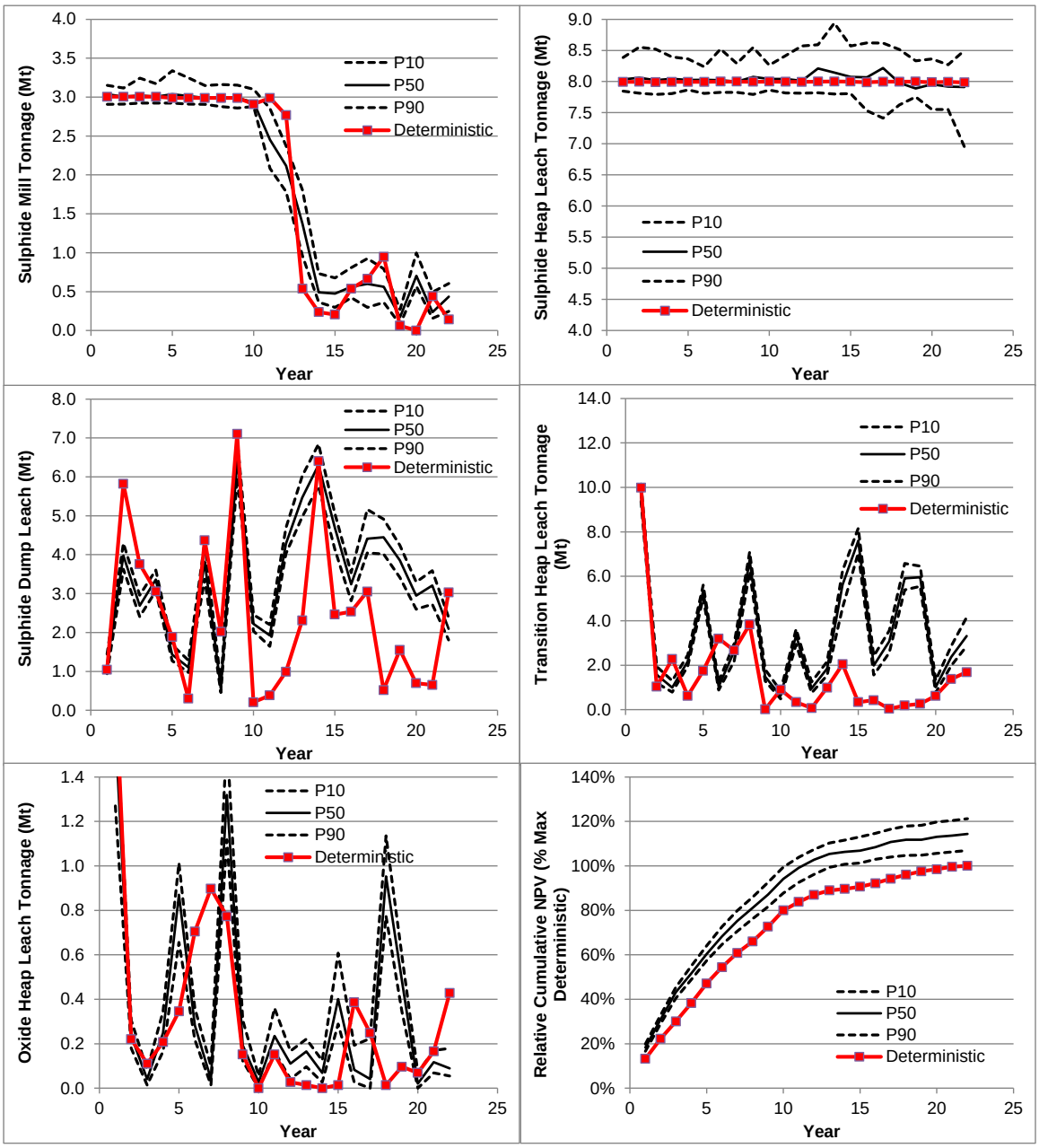

Figure 5: Comparison of tonnage and NPV profiles generated using deterministic optimization and stochastic optimization with the proposed methodology.

deterministic schedule and the stochastic global asset optimizer are generated using the same mathematical model, and this phenomenon did not happen in the supply chain optimization solution in Figure 4, despite the fact that there is a substantial shortage of material for the sulphide heap leach. It is more likely that the lack of material sent to the transition heap leach is only a result of the production scheduling rather than a sub-optimal destination policy. The risk profiles of the oxide heap leach tonnage for the stochastic solution do not change drastically from that of Figure 4; on average, this destination receives the smallest quantity of material, hence doesn't have a substantial impact on the NPV. Finally, Figure 5 shows that the expected NPV of the stochastic solution obtained by the global optimizer is 14.2% higher than that of the deterministic model, and 15% higher than the expected value of the risk analysis of the deterministic

solution. The stochastic solution therefore not only reduces the risk of quantities of materials going to the key profit-generating destinations, but the solution also has a substantially higher value than the deterministic solution.

Figure 6 shows a cross-section of the mine production schedule for both the deterministic and stochastic optimizers. For the deterministic design, it is noted that the schedule is smooth and benchwise – a result of using Whittle's output sequence as a starting sequence for the proposed method. The stochastic schedule shows some drastic differences; the schedule is much less smooth – a common result from many optimization formulations that have difficulties accommodating smoothness, and, moreover, the shape of the final pit is substantially different. The size of the stochastic solution's ultimate pit is 22% larger in tonnage than that of the deterministic pit – a substantial increase in size that indicates better utilization of the non-renewable resource.

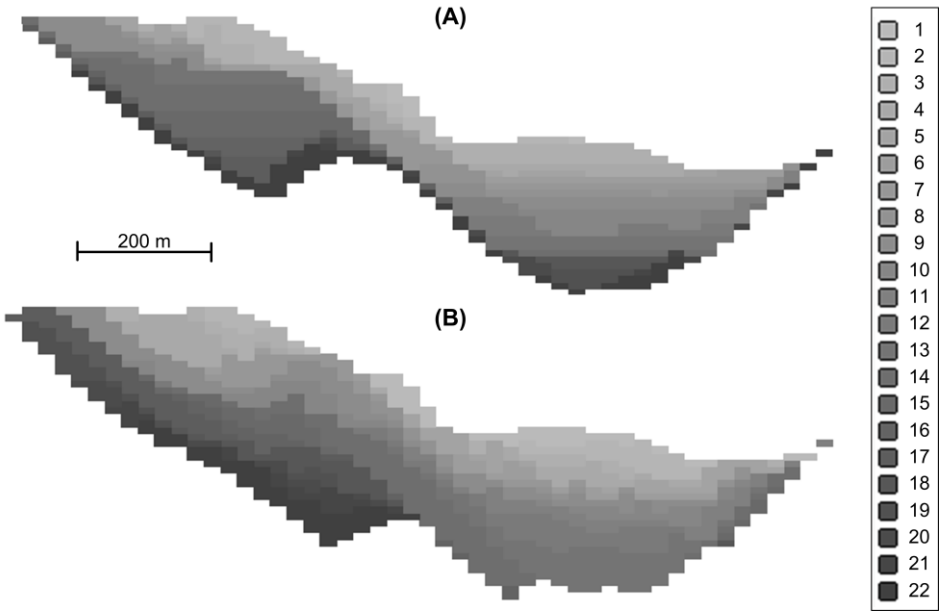

Figure 6: Cross-section of the (A) deterministic and (B) stochastic production schedules.

Figure 7 shows the risk profiles for the sulphide mill tonnage and sulphide heap leach tonnages after performing a sensitivity analysis of the stochastic solution with the remaining 10 simulations that were not during optimization. Despite the risk profiles being "tight" for the 40 input simulations, it is not as robust for the remaining 10 unused simulations, which indicates that the stochastic solution is sensitive to the input simulations. Specifically, the sensitivity analysis indicates an 8% risk and 5% risk of being above or below the sulphide mill tonnage and sulphide heap leach tonnage targets, respectively, but still meet the target capacity on average. The NPV, whose graph has been omitted for brevity, remains relatively stable, with only a 2% decrease from what the stochastic solution originally indicated. Admittedly, the drastic change in risk profiles is an unexpected result. Further investigation shows that this result is not the result of a limitation of the optimizer, but is rather the result of the clustering in the proposed method. The ability to make production scheduling decisions with destination policies effectively permits the optimizer to find block and policy configurations that are similar to making a block's destination decisions for each simulation rather than tying the simulations together through the cluster policies. Future work will seek to improve the solution sensitivity and robustness by looking into innovative ways to penalize these fine-scale changes to the solution. Regardless of this shortcoming, the stochastic solution still provides a stable quantity of material to the sulphide mill and sulphide heap leach, and the increased NPV over the deterministic solution is not sacrificed.

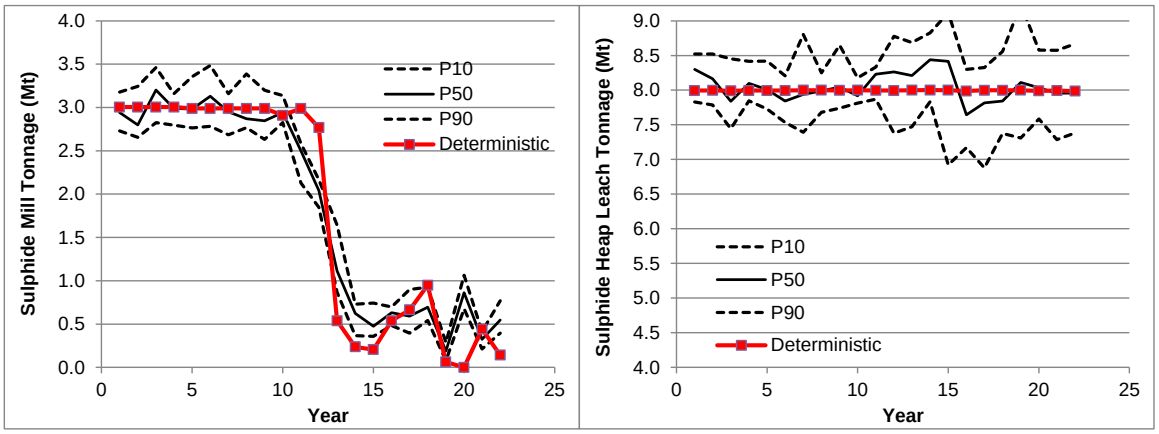

Figure 7: Sensitivity analysis of stochastic solution with 10 unused simulations.

4 Conclusions

This paper presents a simulation-optimization framework for global asset optimization of mining complexes under uncertainty, whereby the solutions give robust long-term open-pit mine production schedules and destination policies. The proposed framework permits a high-degree of flexibility and detail in modelling the mining complex, including the opportunity to integrate non-linear relationships that are generally ignored in existing models because of the challenges associated with optimization. The mathematical formulations can be generalized as a mixed integer non-linear stochastic programming problem, where the first-stage decisions are the production schedules for the mines along with the destination policies, and the recourse decisions decide how to best use the processing streams and destinations in order to maximize the value of the material that has been extracted. The optimizer uses a hybrid metaheuristic comprised of particle swarm optimization and a modified simulated annealing optimizer, whereby the particle swam optimizes the destination policies and processing streams and the simulated annealing optimizes the long-term production schedules and destination policies.

The method is tested on a copper-gold mining complex. Experimental results show a 3.5% and 2.7% average reduction in risk for not meeting production targets at the sulphide mill and sulphide heap leach destinations, respectively. Additionally, the stochastic solution indicates a 14.2% higher net present value and 22% increase in total tonnage for the mining complex than the deterministic solution, thus better utilization of the non-renewable natural resource. Future work will focus on how to improve the clusterings used to define the destination policies through metaheuristic clustering, with the aim of improving both economic value and solution robustness. Given that the proposed method seeks to generate a single, robust set of destination policies, it is of interest to investigate the use of multistage stochastic optimization in order to permit adaptive policies under both supply (geological) and demand (metal price) uncertainty, which will likely lead to higher economic value.

References

Albor, F. and Dimitrakopoulos, R. (2010) Algorithmic approach to pushback design based on stochastic programming: method, application and comparisons. IMM Transactions, Mining Technology, 119(2), 88–101.

Arthur, D. and Vassilvitskii, S. (2007). k-means++: the advantages of careful seeding. In Proceedings of the Eighteenth Annual ACM-SIAM Symposium on Discrete Algorithms. 1027–1035.

Benndorf, J. and Dimitrakopoulos, R. (2009) Stochastic long-term production scheduling of iron ore deposits: Integrating joint multi-element geological uncertainty. In Proceedings of Orebody Modelling and Strategic Mine Planning 2009, AusIMM, 155–164.

Birge, J.R., Louveaux, F. (1997) Introduction to stochastic programming. Springer Series in Operations Research, Berlin.

Bley, A., Gleixner, A.M., Koch, T., Vigerske, S. (2012) Comparing MIQCP solvers to a specialized algorithm for mine production scheduling. Modeling, Simulation and Optimization of Complex Processes, 25–39.

Bodon, P., Fricke, C., Sandeman, T., Stanford, C. (2009) Combining optimisation and simulation to model a supply chain from pit to port. In Proceedings of Advances in orebody modelling and strategic mine planning: Old and new dimensions in a changing world, AusIMM Spectrum Series 17, 1st Edition. 277–283.

Boland, N., Dumitrescu, I., Froyland, G. (2008) A multistage stochastic programming approach to open pit mine production scheduling with uncertain geology. Working paper. Retrieved November 25, 2010, http://www.optimization-online.org/DB_FILE/2008/10/2123.pdf.

Chanda, E. K. (2007) Network linear programming optimization of an integrated mining and metallurgical complex. In Proceedings of Orebody modelling and strategic mine planning: Uncertainty and risk management models, AusIMM Spectrum Series 14, 2nd Edition. 149–155.

Cormen, T.H., Leiserson, C.E., Rivest, R.L. (2009) Introduction to Algorithms (3rd ed.). MIT Press, 1312 p.

Das, S., Abraham, A., Konar, A. (2009) Metaheuristic clustering. Studies of Computational Intelligence (178). Springer, 254 p.

De Frietas Silva, M., Lamghari, A., Dimitrakopoulos, R. (2013) Network-flow based algorithm applied to the stochastic open-pit mine production scheduling of a multi-processor gold mine. COSMO Report No. 7, 184–213.

Dimitrakopoulos, R., Ramazan, S. (2004) Uncertainty based production scheduling in open pit mining. SME Transactions, 316, 106–112.

Geman, S., Geman, D. (1984) Stochastic relaxation, Gibbs distribution and the Bayesian restoration of images. IEEE Trans. On Pattern Analysis and Machine Intelligence, PAMI-6(6), 721–741.

Goodfellow, R., Dimitrakopoulos, R. (2012) Mining supply chain optimization under geological uncertainty. COSMO Report No. 6, 1–43.

Goodfellow, R., Dimitrakopoulos, R. (2013) Algorithmic integration of geological uncertainty in pushback design for complex multiprocess open pit mines. IMM Transactions, Mining Technology, 122(2), 67–77.

Hoerger, S., Bachmann, J., Criss, K., Shortridge, E. (19991) Long term mine and process scheduling at Newmont's Nevada operations. In Proceedings of the 28th APCOM Symposium, 739–748.

Hoerger, S., Hoffman, L., Seymour, F. (19992) Mine planning at Newmont's Nevada Operations, Mining Engineering, 51(10), 26–30.

Jewbali, A. (2006) Modelling geological uncertainty for stochastic short-term production scheduling in open pit metal mines. PhD thesis, University of Quensland, Brisbane, Australia. 186 p.

Kennedy, J., Eberhart, R.C. (1995) Particle swarm optimization. Proceeding of IEEE Int'l Conf. on Neural Networks IV, 1942–1948.

Khalokakaie, R., Dowd, P.A., Fowell, R.J. (2000) Lerchs-Grossmann algorithm with variable slope angles. IMM Transactions, Mining Technology, 109(2), 77–85.

Kirkpatrick, S., Gelatt, C.D., Vecchi, M.P. (1983) Optimization by simulated annealing, Science, 220(4598), 671–680.

Lamghari, A., Dimitrakopoulos, R. (2012a) A diversified Tabu search approach for the open-pit mine production scheduling problem with metal uncertainty. European Journal of Operational Research, 222(3), 642–652.

Lamghari, A., Dimitrakopoulos, R. (2012b) A network-flow based algorithm for scheduling production in multi-processor open-pit mines accounting for metal uncertainty. COSMO Report No. 6, 241–284.

Lane, K.F. (1988) The economic definition of ore – cur-off grades in theory and practice. Mining Journal Books, 1–156.

Leite, A., Dimitrakopoulos, R. (2007) A stochastic optimization model for open pit mine planning. Application and risk analysis at a copper deposit. IMM Transactions, Mining Technology, 116(3), 109–118.

Lloyd, S.P. (1982) Least squares quantization in PCM. IEEE Transactions on Information Theory, 28(2), 129–137.

Menabde M., Froyland G., Stone P., Yeates, G. (2007) Mining schedule optimization for conditionally simulated orebodies. In Proceedings of Orebody modelling and strategic mine planning: Uncertainty and risk management models, AusIMM Spectrum Series 14, 2nd Edition, 379–384.

Montiel, L., Dimitrakopoulos, R. (2012) An extended stochastic optimization method for multi-process mining complexes. COSMO Report No. 6, 67–95.

Monkhouse, P.H.L., Yeates, G.A. (2007) Beyond nave optimization. In Proceedings of Orebody modelling and strategic mine planning: Uncertainty and risk management models, AusIMM Spectrum Series 14, 2nd Edition, 3–8.

Ramazan, S., Dimitrakopoulos, R. (2004) Extension of SIP modelling for long term production scheduling with stochastically designed stockpiles and multiple ore processors. Confidential Report N-6003-1 for ARC Linkage Grant #LP0211446, 1–90.

Ramazan, S., Dimitrakopoulos, R. (2012) Production scheduling with uncertain supply: A new solution to the open pit mining problem. Optimization and Engineering, in press.

Rendu, J.M. (2008) An introduction to cut-off grade estimation. Society for Mining Metallurgy and Exploration, 1–106.

Sandeman, T., Fricke, C., Bodon, P., Stanford, C. (2010) Integrating optimization and simulation – a comparison of two case studies in mine planning. In Proceedings of 2010 Winter Simulation Conference, 1898–1910.

Whittle, G. (2007) Global asset optimisation. In Proceedings of Orebody modelling and strategic mine planning: Uncertainty and risk management models, AusIMM Spectrum Series 14, 2nd Edition. 331–336.

Whittle, J. (2009) The global optimizer works – what next? In Proceedings of Advances in orebody modelling and strategic mine planning: Old and new dimensions in a changing world, AusIMM Spectrum Series 17, 1st Edition. 3–5.

Yanbin, C. (2008) Application of simulated annealing particle swarm optimization algorithm in power coal blending optimization. In Proceedings of the 4th International Conference on Wireless Communications, Networking and Mobile Computing, 1–4.